Plant, Cell and Environment (2016) doi: 10.1111/pce.12855

Original Article

Temperature-compensated cell production rate and elongation zone length in the root of *Arabidopsis thaliana*†

Xiaoli Yang[1,2], Gang Dong[1], K. Palaniappan[3], Guohua Mi[2] & Tobias I. Baskin[1]

[1]*Biology Department, University of Massachusetts, Amherst, 01003, MA, USA,* [2]*College of Resources and Environmental Science, China Agricultural University, Beijing, 100193, China and* [3]*Computer Science Department, University of Missouri, Columbia, 65211, MO, USA*

ABSTRACT

To understand how root growth responds to temperature, we used kinematic analysis to quantify division and expansion parameters in the root of *Arabidopsis thaliana*. Plants were grown at temperatures from 15 to 30 °C, given continuously from germination. Over these temperatures, root length varies more than threefold in the wild type but by only twofold in a double mutant for *phytochrome-interacting factor 4 and 5*. For kinematics, the spatial profile of velocity was obtained with new software, Stripflow. We find that 30 °C truncates the elongation zone and curtails cell production, responses that probably reflect the elicitation of a common pathway for handling severe stresses. Curiously, rates of cell division at all temperatures are closely correlated with rates of radial expansion. Between 15 to 25 °C, root growth rate, maximal elemental elongation rate, and final cell length scale positively with temperature whereas the length of the meristem scales negatively. Non-linear temperature scaling characterizes meristem cell number, time to transit through either meristem or elongation zone, and average cell division rate. Surprisingly, the length of the elongation zone and the total rate of cell production are temperature invariant, constancies that have implications for our understanding of how the underlying cellular processes are integrated.

Key-words: cell division rate; computer vision; elemental elongation rate; kinematic analysis; phytochome-interacting factor; radial expansion; root growth; Stripflow.

INTRODUCTION

For plants, acclimation often features growth. Over a lifetime, a plant may grow hundreds or even thousands of organs – shaped, sized, and differentiated in response to the environment. In contrast to their supposed immobility, plants grow through their environment with astonishing plasticity (Sultan 2000).

Correspondence: T. Baskin. Fax: +1-413-545-3243; e-mail: baskin@umass.edu

†*This paper is dedicated to the memory of Prof. Zygmunt Hejnowicz (1929–2016), a kinematic pioneer.*

Growth and its components are studied tractably in roots. These organs grow rapidly and indeterminately and are organized more or less one-dimensionally. High-resolution study still requires working with the root out of soil, raising the question of physiological relevance; nevertheless, roots grow vigorously on artificial substrates and respond eagerly to perturbations, supporting their use for gleaning basic knowledge. In due course, models and hypotheses thus generated can be tested under more naturalistic conditions.

To understand growth acclimation in roots, we chose to vary the environment by changing the temperature. Perhaps second only to light in its importance as an environmental variable, temperature fluctuates continually and affects the plant's every atom. Responses to temperature cover a spectrum from chilling to heat shock. Here, we sought to avoid extremes and instead to focus on moderate temperatures. Extreme heat or cold elicit pathways dedicated to minimizing or mitigating injury; in contrast, moderate temperatures alter developmental and physiological processes, but neither damage the plant nor strongly decrease fitness. Insofar as we are interested in learning how the root alters its growth rate to explore its environment optimally, moderate temperature changes seem useful as a perturbation, occurring ubiquitously and evoking substantial responses.

Over moderate temperatures, various growth parameters depend on the product of temperature and time (Tardieu & Granier 2000). In the leaves of maize (Ben-Haj-Salah & Tardieu 1995), sunflower (Granier & Tardieu 1998) and *Arabidopsis thaliana* (Granier *et al.* 2002), the rates of cell division and elemental expansion, as well as the durations over which these processes occur, scale linearly with temperature and have a common intercept. This is true both for experiments in growth chambers (i.e. constant temperatures) and in the field (i.e. freely fluctuating temperatures). These linear relationships show that temperature affects growth parameters comparably; or to put it another way, leaf development at different temperatures becomes invariant when plotted against the product of temperature and time. This scaled axis (i.e. temperature x time) is referred to as *thermal time* (Trudgill *et al.* 2005).

When this analysis is extended to encompass a greater range of temperatures and processes, the full temperature-response curve becomes curvilinear (thus not strictly proportional to the product of temperature and time); nevertheless, the

© 2016 John Wiley & Sons Ltd

similarity among growth-related responses remains (Parent *et al.* 2010). In maize, full temperature-response curves are strikingly similar for many growth-related processes, processes that include not only rates of elongation and cell division, but also germination and leaf initiation (Parent & Tardieu 2012). Notably, the data come from various laboratories and include processes with duration ranging from minutes to weeks. Because the shape of the temperature-response curve for these growth-related responses differs from that for photosynthesis or for the activity of various enzymes assayed in vitro, Parent *et al.* (2010) hypothesized that the commonality among growth-related responses to temperature arises from a common pathway for regulation.

Largely absent from the aforementioned analysis are data for roots. While it is tempting to argue that the simplification of thermal-time (or related) scaling is so profound that it must apply to every plant organ, roots differ from leaves in potentially relevant ways. Firstly, leaves grow determinately and mature leaf area is optimized for photosynthesis; in contrast, roots grow indeterminately and root length is not particularly constrained. Secondly, leaf temperature changes on a scale of minutes as clouds and air currents come and go; in contrast, root temperature is comparatively stabilized by soil. Therefore, there is no reason to assume a priori that thermal time applies to roots.

Certainly, root elongation rate appears to follow the common pattern of temperature response (Parent & Tardieu 2012). However, root elongation rate is the integral of several component processes, including cell division, elemental (sometimes called 'cell') elongation, and the durations over which those processes take place. That these component processes do respond to temperature like leaves might be inferred from studies of the maize root transferred to a series of temperatures between 16 and 29 °C (Pahlavanian & Silk 1988), where elemental elongation rate and its duration scaled with temperature. However, more recently, a contrasting pattern was reported for maize roots grown at distinct temperatures for many days (Nagel *et al.* 2009) leading the authors to suggest that the results of Pahlavanian and Silk (1988) apply specifically to transient responses. As for cell division, in the maize root, cell production appears to scale with temperature (Erickson 1959; Silk 1992) but neither study was particularly complete. While cell division in roots as a function of temperature has long been studied with cytological methods (reviewed in Grif *et al.* 2002), those papers typically include little if any companion data on elongation and the use of cytological methods for quantifying division parameters has been criticized (Green 1976; Webster & MacLeod 1980; Baskin 2000; Fiorani & Beemster 2006) and in some cases demonstrated to give results at odds with direct kinematic measurement (Tardieu & Granier 2000).

Here, we investigate how moderate temperatures alter growth processes in the root of *A. thaliana*. We use this species because the shape and size of the root are particularly favourable for kinematic analysis, a method that allows key growth parameters to be characterized non-invasively and with good spatial and temporal resolution (Beemster & Baskin 1998; Fiorani & Beemster 2006). We characterize steady-state behaviour to establish baseline behaviour and to avoid the complexity of transient responses. We report that while elongation appears to change linearly over a moderate temperature range, indicating the applicability of thermal time, division parameters respond distinctly. In addition, from 15 to 25 °C, both the length of the elongation zone and total cell production rate are essentially insensitive to temperature. These results reveal an unexpected plasticity in the root's responses to temperature.

MATERIALS AND METHODS

Plant growth and experimental treatments

Arabidopsis thaliana (L.) Heynh, Columbia, was the background for all material. Some experiments used a line expressing a green fluorescent protein (GFP)-tagged plasma membrane protein (GFP-LTI6a; Grebe *et al.* 2003) or a double mutant in *phytochrome-interacting factors 4* and *5* (*pif4/pif5*; Lorrain *et al.* 2008). Seeds were stored at 4 °C. At day 0, they were surface sterilized in 70% ethanol for 5 min, followed by 25% bleach for 5 min, and rinsed 6 times in sterile water. Seeds were plated on agar-solidified medium containing a modified Hoagland solution (Baskin & Wilson 1997) and 1% sucrose in 10 cm round Petri dishes, which were placed vertically in a growth chamber at the indicated temperature under constant yellow light ($100\,\mu mol\,m^{-2}\cdot s^{-1}$) as described by Rahman *et al.* (2007). Constant light was used to avoid the pronounced diurnal oscillation in root growth rate that occurs under a photoperiod (Yazdanbakhsh & Fisahn 2010). For kinematic experiments, to enhance image quality and minimize temperature transients when moving plates, we inserted seeds into the agar, which led the root to grow within the agar, rather than on the surface. In preliminary experiments, we determined that root elongation rate within and on the agar surface were similar at all of the tested temperatures. For kinematic analysis at each temperature, from three to five roots were assayed on a given day and a total sample size ranging from 11 to 15 roots was built up from three replicate experiments.

Imaging for velocity and cell length

Prior to running kinematic experiments, we obtained the time course of root growth for each studied temperature by running a 'ticking' experiment, as described by Baskin and Wilson (1997). Briefly, the position of the root tip was scored with a razor blade on the back of the Petri dish once per day at a noted time; at the end of the experiment, the dishes were scanned, and the length along the roots between score lines was measured by using ImageJ (Rasband 2015).

For the determination of the root's velocity profile, a plate was removed from the growth chamber and placed on the stage of a horizontal compound microscope, and a root was imaged through a 20X objective and a CCD camera (Model 18 Spot Insight, Diagnostic Imaging) with infrared light. The position of the root tips on the plate had been scored over the preceding 2 days, allowing a root to be selected for imaging that was growing near the average rate. The stage position was controlled electro–mechanically (8200 Inchworm Controller, EXFO, Quebec, Canada). As needed for analysis (see below), a pair of

images was obtained over a 30 s interval, except for experiments at 30 °C for which a 60 s interval was used. The stage was translocated by a defined amount to an adjacent region of the growth zone and another image pair obtained, continuing until the complete growth zone was spanned (4–7 image pairs in total).

To minimize temperature changes, we transferred plates from the growth chamber to the microscope (a distance of ~50 m) in an insulated box containing a large metal mass that had been equilibrated in the growth chamber, and only one root was imaged per plate. Additionally, the temperature in the microscope room was adjusted to match the growth chamber temperature (exact match was not possible for 15 and 30 °C).

Directly after image capture, the root was removed from the agar, and fluorescence from GFP-LTI6a was imaged through a scanning confocal fluorescence microscope (Nikon Eclipse TE-2000S) with a 40X, 1.0 NA objective. For seedlings grown at 25 and 30 °C, GFP fluorescence was weak or invisible; therefore, for those temperatures, after imaging for velocity determination, the root was incubated in propidium idiode solution (30 μM) for 5 min, rinsed with distilled water and imaged through the confocal.

Velocity profile determination

For each root, the velocity profile was obtained algorithmically by means of new software called Stripflow. This runs in MATLAB (MathWorks, Natick, MA, USA), as described further in the supporting information. Briefly, Stripflow takes advantage of the fact that the displacements of interest are parallel to the long axis of the root. For each pixel along the root's midline, starting from the quiescent centre, it estimates the velocity of a strip oriented perpendicular to the local midline and reports the parallel component of velocity. For the experiments here, strip width was 40 pixels (about 20 μm). The origin of the profile is the quiescent centre, selected by eye as adjacent to the last tier of starch grains within the root cap. A limitation of the software is that midline points are determined by eye; in tests, we found that the velocity profiles are not particularly sensitive to the choice of midline, provided that extreme choices are avoided.

Kinematic calculations

Calculations were applied to data for individual roots, essentially as described previously (Beemster & Baskin 1998). Raw velocity and cell length profiles were fitted to overlapping polynomials by means of a non-linear curve fitting routine Locpoly written in R (Nelissen *et al.* 2013; The R Project for Statistical Computing, https://www.r-project.org) and fitted points obtained at 25 μm intervals. The spatial profile of elemental elongation rate, r (h^{-1}), given as

$$r = dV/dx \tag{1}$$

where V is velocity and x is distance from the quiescent centre, was obtained from the derivative of the fitted velocity profile.

To obtain elemental rates of radial expansion, we measured root diameter in the same images used to obtain the velocity profile. Diameter was measured manually in IMAGEJ at 50 μm intervals, starting in the root cap and with the quiescent centre taken as $x = 0$. Elemental radial expansion rate, W (h^{-1}), was obtained as follows:

$$W = (1/R)(dR/dx)(V) \tag{2}$$

where R is the radius of the root (Silk & Abou Haidar 1986). Although strictly speaking, W represents expansion in the circumferential direction (i.e. along the outer surface of the root), which need not exactly equal expansion along a radius (Liang *et al.* 1997), we refer to W as (elemental) radial expansion for convenience. The second term (i.e. dR/dx) was evaluated by using three-point differentiation formula (Erickson 1976). The full expression for W contains a time-dependent term (i.e. dW/dt); however, this term was negligible throughout the meristem based on measuring, for each temperature, diameter as a function of position over several days.

The number of cells moving past any position per unit time is cell flux, F (cells h^{-1}) and is given by the ratio of velocity and cell length, L, at that position:

$$F = V/L \tag{3}$$

Cell flux was obtained from the fitted curves. The local rate of cell production, P (cells μm^{-1} h^{-1}) is then calculated as follows:

$$P = (\delta F/\delta x) + (\delta \rho/\delta t) \tag{4}$$

where ρ is the density of cells (taken as the reciprocal of cell length in a linear system like the root). Because the magnitude of the second term was small to negligible, it was set to zero. Plots of F versus x were smoothed and differentiated by using five-point formulae (Erickson 1976). Local cell production rate defined thus is unusual, insofar as it reflects proliferation activity on a per unit length basis. To convert these values to the more conventional cell division rate, D (proliferation on a per cell basis), we used the following relation:

$$D = (P)(L) \tag{5}$$

The number of cells in the meristem N_{div} was obtained by summing the number of cells based on the fitted profile of cell length from the quiescent centre to the position where cell production rate first reached zero. Average cell division rate of the meristem, $\overline{D}$ (h^{-1}), was calculated as final cell flux, F_f, divided by the number of dividing cells:

$$\overline{D} = F_f/N_{div} \tag{6}$$

Average cell cycle duration, $\overline{T_c}$ (h), was calculated as follows:

$$\overline{T}_c = 1n(2)/\overline{D} \tag{7}$$

The residence time of a transverse cell wall in the meristem, T_{div}, was estimated from

$$T_{div} = \overline{T}_c \text{ x } \log_2(N_{div}) \tag{8}$$

To define the length of the elongation zone, we estimated the positions of its shootward and rootward boundaries from the velocity profile. The shootward boundary (i.e. end of the

© 2016 John Wiley & Sons Ltd, *Plant, Cell and Environment*

growth zone) was where the velocity profile first reached 95% of maximum. The rootward boundary was defined as the first transition point ('c1') in the flexible logistic function invented by Peters and Baskin (2006) to handle growth curves with bi-linear character. The raw velocity profile was fitted to the function by means of a non-linear curve fitting routine written in R.

The number of cells in the elongation zone was obtained by integrating the number of cells between shootward and rootward boundaries, based on the fitted profile of cell length. The time a particle requires to transit the elongation zone, T_{el}, was estimated from

$$T_{el} = Int + (25) \sum_{x=rb}^{sb} 1/V(x) \quad (9)$$

where *rb* and *sb* represent the rootward and shootward elongation-zone boundaries, respectively, and *Int* represents the time to go between each actual boundaries and the nearest point at 25 μm. The same approach was used to define cell number and transit time between the end of the meristem and the start of the elongation zone.

RESULTS

Root elongation rate over time

To study how temperature influences root growth, we grew *A. thaliana* seedlings between 15 and 30 °C (at 5 °C steps), a range chosen to avoid acute stress. Seeds were germinated and grown at the indicated temperature continuously. Root growth was monitored by marking the position of the root tip (see Section on Materials and Methods). After 10 days, root length was roughly proportional to temperature between 15 and 25 °C, but fell well short of this trend at 30 °C (Fig. 1). Proportionality between growth and temperature might indicate a direct influence of temperature on a rate-limiting reaction that loosens the cell wall (Pritchard *et al.* 1990; Nakamura *et al.* 2002). To examine regulation, we compared the response of the wild type with that of a double mutant in *phytochrome interacting factors4* and *5* (*pif4/pif5*). These transcription factors, although discovered by virtue of their action in phytochrome-mediated responses, have been implicated in coordinating various responses of the shoot to elevated temperature (Koini *et al.* 2009; Kumar *et al.* 2012; Franklin *et al.* 2014). The roots of the double mutant responded to temperature, but compared with those of the wild type, they responded weakly (Fig. 1). This was true not only for increasing growth at 20 and 25 °C but also for decreasing at 30 °C. This contrasts with behaviour in the hypocotyl, where elongation in the *pif4* mutant is indistinguishable at a pair of temperatures (22 and 28 °C in Koini *et al.* 2009; 20 and 29 °C in Stavang *et al.* 2009). These data support the notion that growth responses to temperature are at least partly indirect; however, the data suggest that regulation differs between shoots and roots.

Because *A. thaliana* seedling roots grow faster over time (Beemster & Baskin 1998), we characterized the time course of root elongation (Fig. 2). Root growth rate accelerated at all temperatures but accelerated faster with increasing temperature between 15 and 25 °C. At all temperatures, root elongation rate eventually plateaued. Similar to root length at day 10, the growth-rate plateau was more or less proportional to temperature between 15 and 25 °C; however, at 30 °C, the plateau growth rate was lower even than at 15 °C, suggesting a distinct response.

For the kinematic analysis, we report data for the days indicated by the arrows (Fig. 2), a time when root elongation rate at each temperature was at a plateau or nearly so. In this way, roots are compared at or near steady state, which simplifies

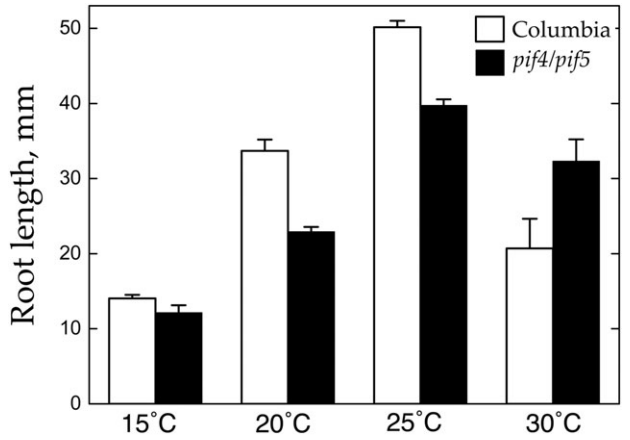

Figure 1. Root length as a function of temperature compared between wild type and *pif4/pif5*. Root length was measured on day 10. Bars plot mean ± SE for three replicate plates, with 6–8 seedlings per plate.

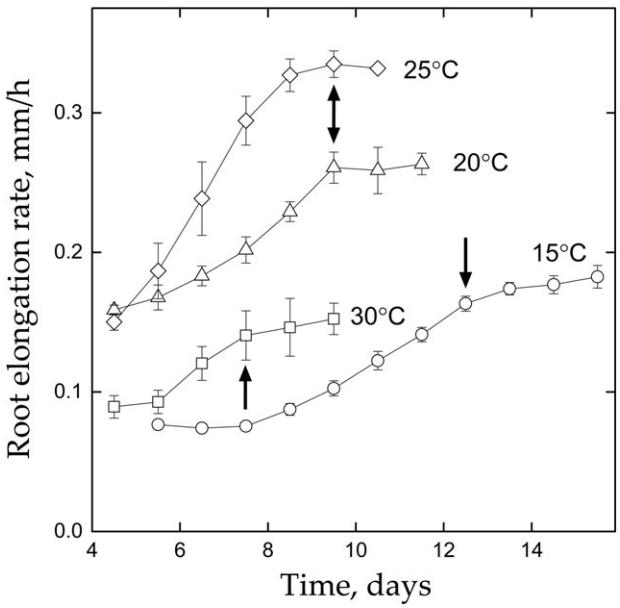

Figure 2. Time course of primary root elongation at different temperatures. Symbols plot mean ± SE of three replicate experiments, each with three plates of six seedlings per plate. Root length was recorded daily, and the rate plotted at the midpoint. Arrows show the time when observations for kinematics were made (on day 12 for 15 °C, day 9 for 20 and 25 °C, and day 7 for 30 °C). Time 0 is when stratified plates were moved into the chamber.

© 2016 John Wiley & Sons Ltd,

the analysis and minimizes potential complications from the developmental acceleration of growth rate. When roots were examined on the indicated days, the elongation zone appeared qualitatively similar in length from 15 to 25 °C and became shorter at 30 °C; whereas, the meristem appeared to shorten with temperature throughout the studied range (Fig. 3). Along with meristem length, root diameter also appeared to decrease with temperature. These appearances were verified and extended with kinematic analysis.

Determination of the velocity profile with stripflow

Kinematic analysis relies on the spatial profile of velocity (Silk 1992). Previously, Palaniappan's group developed software, RootFlowRT, that allows the velocity profile to be obtained from image analysis without marking the root or even opening the Petri dish (van der Weele *et al.* 2003; Palaniappan *et al.* 2004; Dong *et al.* 2006). Here, we accomplish the same task with new software, Stripflow (Supporting information). Stripflow generates velocity profiles that are similar to those of RootFlowRT but are less noisy and require only two sequential input images compared with nine needed by RootFlowRT.

Raw velocity profiles typically had three regions (Fig. 4). In the first (most rootward) region, velocity increased gradually with distance; in the second, velocity increased steeply; in the third, velocity was constant. The first region corresponds to the meristem, although cell division presumably stops rootward of where velocity accelerates; the second corresponds to the elongation zone; and the third corresponds to the maturation zone (constant velocity equals zero elongation) (Fig. 3). To the extent that velocity within the first two regions increases linearly, the elemental elongation rate within each region is constant (van der Weele *et al.* 2003; Peters & Baskin 2006).

Elemental elongation rate

As shown by the error bars, the spatial profile of velocity was reproducible among individuals (Fig. 5a). Consistent with the daily measurements (Fig. 2), final velocity increased linearly with temperature from 15 to 25 °C but fell sharply at 30 °C.

The spatial derivative of the velocity profile represents elemental elongation rate (Fig. 5b). Between 15 and 25 °C, elemental elongation rate, at its peak, appeared roughly proportional to temperature. Within the most rootward region (meristem), elemental elongation rate at 15 and 20 °C were similar and about half that at 25 °C (Fig. 5b inset). From 15 to 25 °C, the length of the growth zone appeared roughly constant; whereas, at 30 °C, the profile of elemental elongation rate was truncated rootward, typical of responses to various kinds of stress (Baskin 2013).

Between 15 and 25 °C, each 5 °C step increased maximal elemental elongation rate to a similar extent (Table 1). To assess

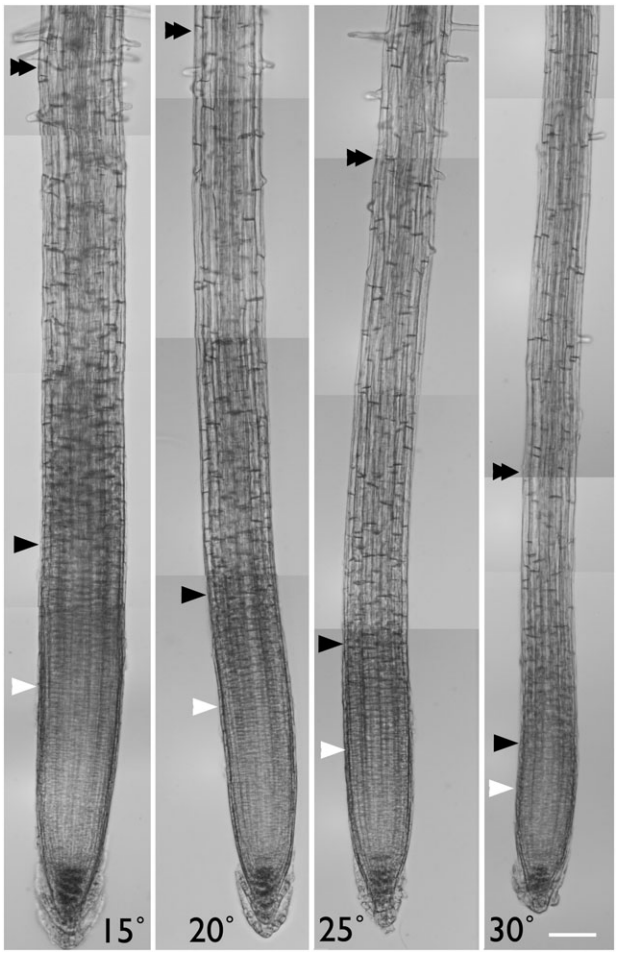

Figure 3. Micrographs from Stripflow input exemplifying morphological effects of the various temperatures. Images are marked to show relevant boundaries, as found for that root (*white arrowhead*: shootward boundary of the meristem; *black arrowhead*: rootward boundary of the zone of elongation; *double arrowhead*: shootward boundary of the zone of elongation). Bar = 100 μm.

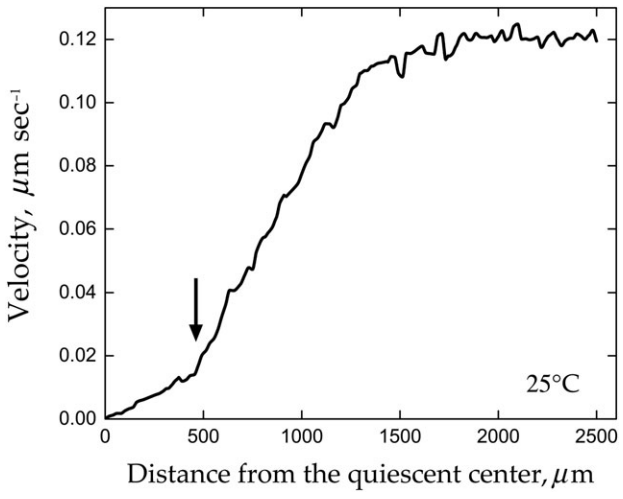

Figure 4. Example of a velocity profile output from the new software, Stripflow. Arrow points to the approximate position of the breakpoint between regions of shallow and steep velocity increase, denoted 'c1' in the bi-linear sigmoid function introduced by Peters and Baskin (2006).

© 2016 John Wiley & Sons Ltd, *Plant, Cell and Environment*

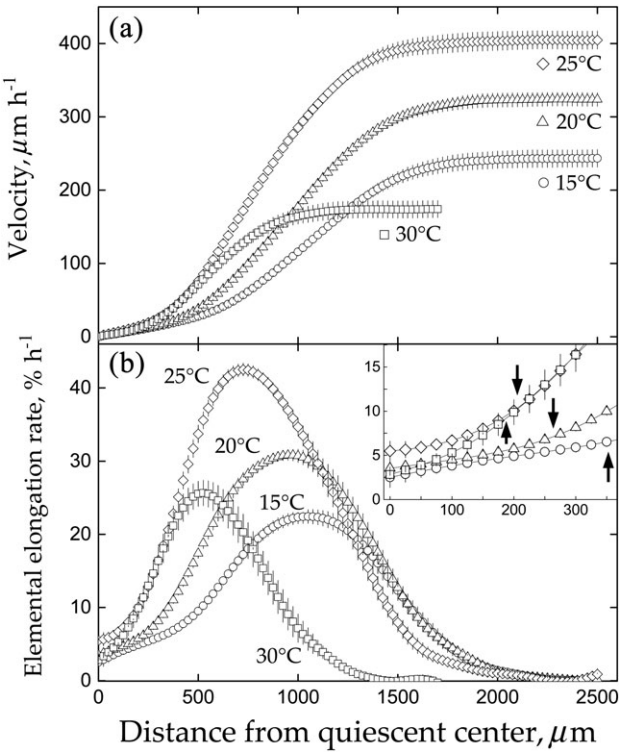

Figure 5. Spatial profiles of velocity (a) and elemental elongation rate (b) at various temperatures. Inset in (b) shows the first few hundred microns of the elemental elongation rate profiles enlarged for clarity; the arrows indicate the approximate average position where cell production rate fell to zero (i.e. the shootward boundary of the meristem). Symbols plot mean ± SE of the individuals sampled on various days, with $n = 13$ at 15 °C, $n = 15$ at 20 °C, $n = 11$ at 25 °C, and $n = 12$ at 30 °C.

the length of the elongation zone, we defined its shootward boundary as the position where velocity attained 95% of its maximum and its rootward boundary as the location separating regions of gradual and steep velocity increase (Fig. 4 arrow; obtained numerically as described in Materials and Methods). The rootward boundary (i.e. the onset of rapid elongation) moved towards the tip by about 125 μm for each 5 °C increase; nevertheless, the total elongation zone length, although shortened at 30 °C, was roughly constant between 15 and 25 °C (Table 1). This constancy occurred under constant temperature, which contrasts the suggestion, made by Nagel *et al.* (2009) for maize, that elongation zone length is stable only transiently in roots responding to a temperature shift. Finally, in contrast to length, the time to traverse the elongation zone decreased by about 1 hour for each 5 °C increase in temperature between 15 and 25 °C. Again, 30 °C differed, shrinking the length of the zone and prolonging the time needed to traverse it. Between 15 and 25 °C, the roughly constant elongation zone length despite the decreased transit time (and increasing cell length, see below), suggests that the zone's length is maintained by a cell-non-autonomous mechanism.

Elemental radial expansion rate

Although elongation accounts for the majority of expansion in the root, radial expansion is finite and root diameter is regulated physiologically. Because elemental radial expansion rates are small, rather than measuring them directly, we calculated them from the spatial profiles of velocity and root diameter (Silk & Abou Haidar 1986). Note that because velocity is set to zero at the quiescent centre, our profiles of radial expansion rate begin 50 μm therefrom. In contrast to the maize root (Pahlavanian & Silk 1988), increasing temperature caused roots to become thinner (Fig. 6a), suggesting temperature is inversely correlated with radial expansion rate. However, calculating that rate shows that its relationship to temperature is complex (Fig. 6b). The position where radial expansion rate became negative (i.e. thinning of the root) moved towards the tip in increments that were roughly proportional to the increase in temperature. Insofar as the position where elemental elongation rate accelerates also moved towards the tip with temperature (Fig. 5b; Table 1), the onset of thinning could be a consequence of the stimulated elongation. However, the maximal rate of elemental radial expansion was indistinguishable at 15 and 20 °C, although raised at 25 °C (Fig. 6b). Root diameter can be maximal at 15 °C while radial expansion rate is minimal because radial expansion rate is instantaneous whereas diameter is cumulative; meristem cells at 15 °C expanded radially for a sufficiently longer period than those at 25 °C, more than compensating for their lower rate and thereby generating a wider root.

Table 1. Elongation zone parameters in roots exposed to constant temperatures

Temp °C	Max. elem. elong. rate, % h^{-1}	Transition 1 location, μm	Elongation zone length, μm	Elong. zone traverse time, h	Elong. zone cell number
15	23.2 ± 0.9	676 ± 21	984 ± 35	8.4 ± 0.5	14.3 ± 0.7
20	32.1 ± 1.1	552 ± 20	1084 ± 37	7.4 ± 0.4	11.6 ± 0.7
25	42.8 ± 1	419 ± 11	1015 ± 26	5.8 ± 0.2	10.0 ± 0.6
30	27.7 ± 1.7	333 ± 23	720 ± 44	8.7 ± 0.7	8.1 ± 0.5

Data are mean ± SE. Sample sizes are given in the legend to Fig. 5. Parameters are defined in the Section on Materials and Methods. Briefly, *Max. elem. elong. rate* averages the peak elemental elongation rate; *Transition 1 location* gives the position of the breakpoint between regions of shallow and steep velocity increase, defined by Peters and Baskin (2006) as 'c1'; *Elongation zone length* is defined as the difference between c1 and the position where the fitted velocity profile reached 95% of its maximum; *Elong. zone traverse time* is the time needed by a particle to go from one elongation zone boundary to the other; and *Elong. cell number* records the number of cells in the elongation zone at a given moment.

© 2016 John Wiley & Sons Ltd,

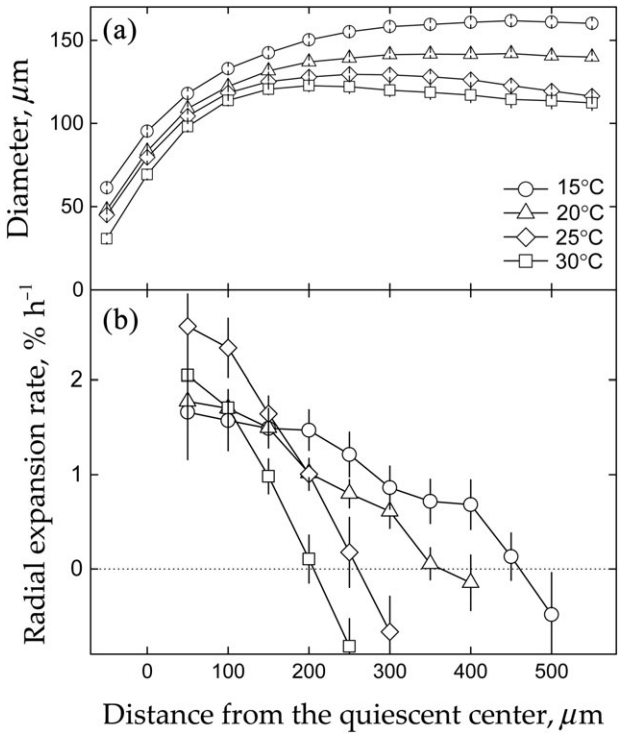

Figure 6. Spatial profiles of (a) root diameter and (b) elemental radial expansion rate. Symbols plot mean ± SE for the same roots used for Fig. 5. Note that radial expansion rate was not calculated for the first 50 μm from the quiescent centre because the calculation uses longitudinal velocity which is zero at $x = 0$.

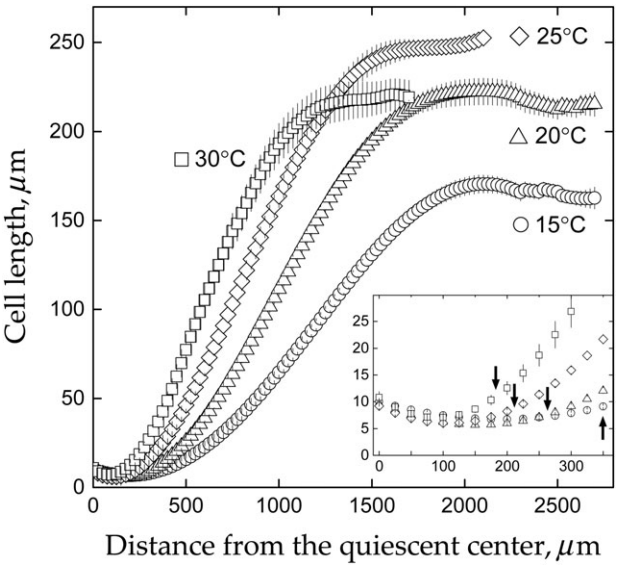

Figure 7. Spatial profile of cell length at various temperatures. Inset shows the first few hundred μm of the cell length profiles enlarged for clarity; the arrows indicate the approximate average position where cell production rate fell to zero (i.e. the shootward boundary of the meristem). Symbols plot mean ± SE for the same roots used for Fig. 5.

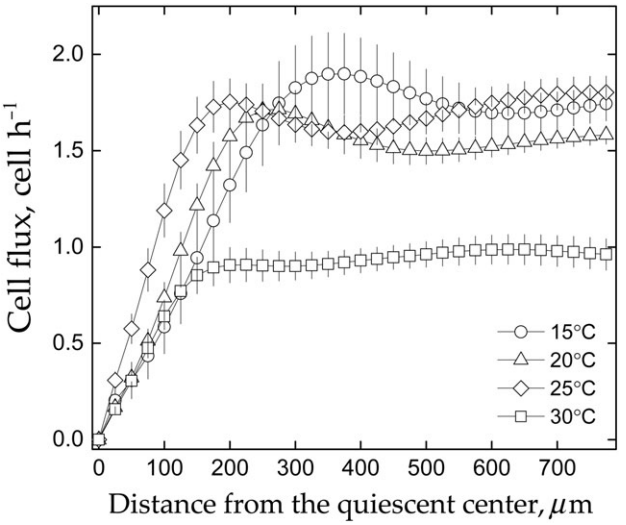

Figure 8. Spatial profile of cell flux at various temperatures. In the ideal case, cell flux would rise to become perfectly constant rather than having the small peak and valley seen here. Because cells are not consumed (i.e. decreasing cell flux), the fluctuations probably arise from the increasing noise as cell length becomes large (and therefore fewer cells per position in one root). Symbols plot mean ± SE for the same roots used for Fig. 5.

Cell division rate

In kinematic analysis, cell division is quantified by comparing the concentration of cells moving past neighbouring points along the root's long axis, with an increase signifying cell division activity between those points. This comparison begins with the spatial profile of cell length (Fig. 7). In the same roots used to measure velocity profiles, we measured the length of cortical cells, because epidermal cells have two cell types, trichoblasts and atrichoblasts, that differ in mean cell length. In general, the plots of cell length versus distance varied among the four temperatures in the position where cell length started to increase steeply, in the slope of the main part of the curve, and in the final plateau value. This variation contrasts with previous reports for roots (Silk 1992) and leaves (Ben-Haj-Salah & Tardieu 1995) of maize where plots of cell length versus distance at different temperatures overlap closely.

Combining, for each root, the profiles of velocity and cell length yields the profile of cell flux (Fig. 8). At all temperatures, these curves rose steeply with position for the first few hundred microns of the root before reaching a plateau value. The plateau cell flux undulated, rather than being strictly constant, probably because as cells get large, there are fewer of them at each position, increasing the uncertainty of the cell length data. Insofar as cells are not destroyed, decreases in cell flux can be only apparent, and the average plateau value can be taken as a reasonable estimate of the total rate of cell production (per file of cortex cells). The plateau was substantially reduced at 30 °C but, surprisingly, showed little if any systematic dependence on temperature between 15 and 25 °C. Invariant final cell flux across a temperature range contrasts with the temperature sensitivity found for *A. thaliana* leaves (Granier *et al.* 2002) and for metaxylem of the maize root (Erickson 1959).

The spatial derivative of cell flux yields a local cell production rate, which has units of cells produced per unit length

© 2016 John Wiley & Sons Ltd, *Plant, Cell and Environment*

and time (Fig. 9a). Between 15 and 25 °C, the maximum rate of local cell production increased, but the position where the rate became zero moved towards the tip, indicating a diminution of the length of the meristem. At 30 °C, the maximum rate fell and the position where it reached zero moved yet closer to the tip. Using the position where cell production rate reached zero to define the shootward boundary of the meristem, we calculated, for each root, the meristem's length, cell number, and traverse time (Table 2). Between 15 and 25 °C, these parameters decreased with increasing temperature. Again 30 °C behaved differently, with the meristem becoming even shorter and containing even fewer cells but nevertheless requiring a greater time to traverse (than at 25 °C). Between 15 and 25 °C, the decreasing length of the meristem contrasts the constancy of elongation-zone length.

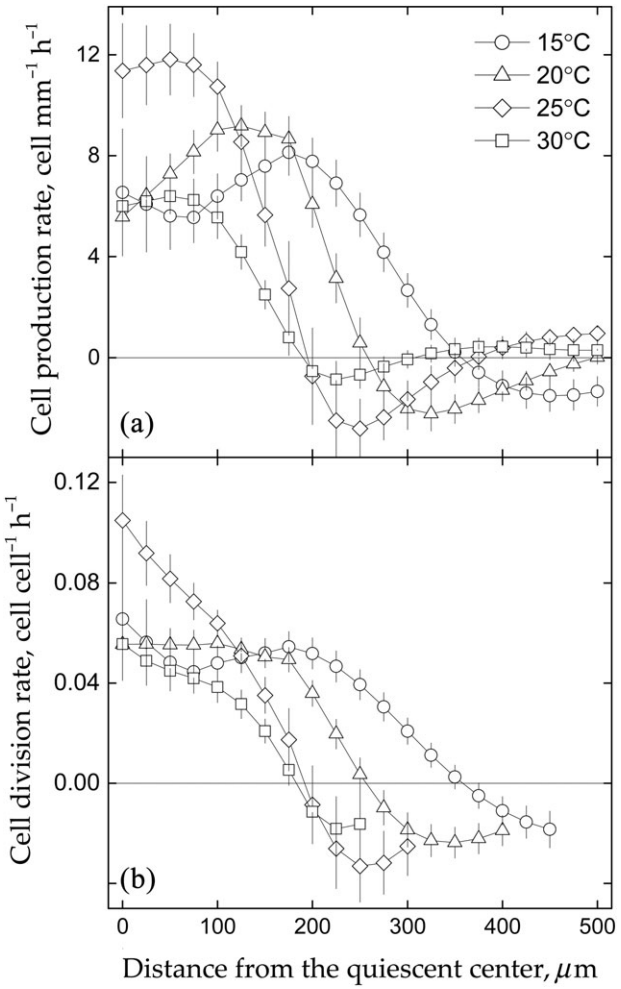

Figure 9. Spatial profiles of (a) cell production rate and (b) cell division rate. Both profiles extend below zero because the profiles of cell flux (Fig. 7) rise to a small peak rather than to a perfect plateau. Symbols plot mean ± SE for the same roots used for Fig. 5.

Converting these data to cell division rates (cells produced per cell and unit time) revealed that cell division rate in the bulk of the meristem appeared to be similar at 15 and 20 °C but notably faster at 25 °C (Fig. 9b). Interestingly, the profiles of cell division rate resembled the profiles of elemental radial expansion rate (Fig. 6b) connecting these distinct processes, perhaps for the first time. That cell division rates appeared similar at 15 and 20 °C was surprising because, like elongation rate, cell division rate typically scales with temperature. To examine cell division rate with an alternative method, we calculated average cell division rate for each root's meristem (Table 2). Confirming the appearance of the spatial profiles, average cell division rate at 15 and 20 °C was indistinguishable and about two-thirds of that rate at 25 °C. Evidently, changes in temperature need not elicit proportional changes in cell division rate and, in the *A. thaliana* root, the mechanisms regulating elongation and division rates in response to temperature appear distinct.

Applicability of thermal time

As described in the *Introduction*, growth in various leaf species tends to scale as the product of time and temperature. For such scaling to occur, the rates and durations of key processes need to change linearly with temperature and have a common *y*-intercept (Granier & Tardieu 1998). Here, to compare the temperature dependence of growth parameters, we expressed them as a percentage of the response at 20 °C, with reciprocals used when needed to plot all parameter values increasing with temperature. Data for 30 °C were excluded.

The parameters grouped in three types (Fig. 10). The first type increased linearly with temperature with similar slope and intercept (Fig. 10a) indicating thermal-time scaling. These parameters included final root velocity and maximum elemental elongation rate. In the second type, the response to

Table 2. Cell division parameters in roots exposed to constant temperature

Temp, °C	Meristem length, μm	Meristem cell number	Meristem traverse time, h	Cell division rate, cell cell^{-1} · h^{-1}	Cell cycle duration, h
15	351 ± 16	46 ± 2	62 ± 5	0.047 ± 0.004	16.1 ± 1.3
20	266 ± 14	40 ± 2	54 ± 4	0.05 ± 0.003	14.7 ± 0.9
25	206 ± 16	30 ± 2	33 ± 3	0.075 ± 0.005	9.8 ± 0.8
30	180 ± 11	23 ± 1	48 ± 4	0.049 ± 0.004	15.1 ± 1.3

Data are mean ± SE. Sample sizes are given in the legend to Fig. 5. Parameters are defined in the Section on Materials and Methods. Briefly, *Meristem length* is the position where local cell production rate became zero; *Meristem cell number* records the number of cells in the meristem at a given moment; *Meristem traverse time* is the time needed by a particle to traverse the meristem; *Cell division rate* gives an average rate calculated from the final cell flux and the number of dividing cells; and *Cell cycle duration* converts the average cell division rate to a doubling time.

© 2016 John Wiley & Sons Ltd,

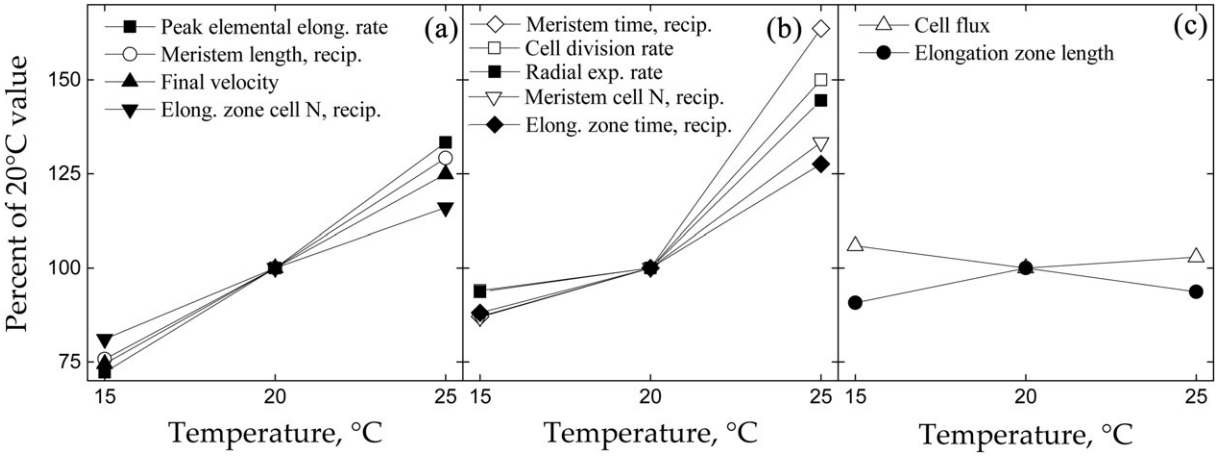

Figure 10. Temperature scaling of selected parameters. Parameters are grouped based on apparent temperature dependency being (a) linear, (b) non-linear, or (c) invariant. Open symbols plot parameters relating to the meristem, filled symbols plot those related to the elongation zone. Parameters that decreased with temperature are plotted as the reciprocal to have a positive correlation with temperature. Original data are given in Tables 1 and 2.

temperature departed from linearity, with the change from 20 to 25 °C tending to evoke a greater increase than evoked by the change from 15 to 20 °C (Fig. 10b). Parameters in this class mainly related to cell division, including cell division rate. For *A. thaliana* leaves, growth parameters scale with thermal time from 6 to 26 °C (Granier *et al.* 2002) suggesting that the behaviour seen here for the root below 20 °C reflects a specific adaptation by the root for growth under prolonged and moderately cool temperatures. Finally, two parameters appeared insensitive to temperature, namely final cell flux and the length of the elongation zone (Fig. 10c). Insofar as achieving temperature invariance requires active compensation, the concomitant stability of final cell flux and elongation zone length is notable.

DISCUSSION

Taking advantage of improved image analysis software, Stripflow, for obtaining the spatial profile of velocity for the growing root, we have characterized growth components of the *A. thaliana* root as a function of temperature between 15 and 30 °C, with the treatment temperature remaining constant from germination onwards. At 30 °C, the elongation zone is truncated rootward and final cell flux is diminished, mimicking responses that occur when roots are exposed to various kinds of stress, including drought, salt, and even chemical inhibitors (Baskin 2013). When exposed to the slightly higher temperature of 33 °C, roots of the Columbia accession of *A. thaliana* stop growing altogether within a day or two after transfer (Baskin *et al.* 1992). Responses at 30 °C probably represent a common pathway for coping with severe stress. In the remaining discussion, we focus on responses to moderate temperature (15 to 25 °C).

Auxin-temperature-elongation syndrome

Increasing temperature in the moderate range increases elongation of the *A. thaliana* hypocotyl, a response driven to a large extent by increased auxin synthesis (Gray *et al.* 1998). Increasing temperature is linked to an increasing auxin supply through a gene for auxin synthesis, *YUCCA8*, being activated by PIF4 (Sun *et al.* 2012). Indeed, PIF4 is increasingly recognized as being part of a regulatory hub for temperature responsiveness (e.g. Kumar *et al.* 2012; Franklin *et al.* 2014; Nieto *et al.* 2015). Our data add temperature regulation in the root to the duties handled by the PIF family of transcription factors.

However in the root, increasing auxin concentration inhibits elongation, which is the opposite of the observed temperature response; therefore, up-regulating auxin supply could mediate the observed growth stimulation in the root only if accompanied by decreased auxin sensitivity. Interestingly, appropriate changes in auxin sensitivity (along with changes in synthesis and transport) have been reported for *A. thaliana* roots experiencing a shift to a higher temperature (Hanzawa *et al.* 2013) and to a lower temperature (Zhu *et al.* 2015). These reports are consistent with auxin playing a major role in mediating the root's response to moderate temperatures. Shifting the temperature down from 22 to 16 °C shortens the root meristem (Zhu *et al.* 2015), and consistently, shifting the temperature up from 23 to 29 °C increases final cell flux (Hanzawa *et al.* 2013); in both reports, the meristem is larger or more active at the higher temperature. That an enlarged root meristem reflects greater auxin levels or responsiveness is consistent with the output of a sophisticated computational model that incorporates known regulatory circuits and cell behaviours (De Vos *et al.* 2014).

Nevertheless, these results linking growth as temperature increases to increased meristem size and auxin response differ from those reported here, where increasing temperature shrinks the meristem (Fig. 9, Table 1) and scarcely changes final cell flux (Fig. 10c). A plausible reason for the different results is that we grew plants at constant temperatures from germination whereas the two cited reports established seedlings at one temperature and then shifted them to the other. Maize roots grown constantly at 16 °C have a growth zone that is substantially shorter than those grown at 25 °C, whereas when they are

© 2016 John Wiley & Sons Ltd,

exposed to temperature-shifts, the length of the growth zone stays constant (Nagel *et al.* 2009) even for a day or two after the temperature shift (Pahlavanian & Silk 1988). Likewise, the roots of a set of about two dozen *A. thaliana* accessions have consistently up-regulated levels of the mitotic cyclin gene, CYCB1;1, when exposed to 10 °C chronically but not when given an initial 1 week pre-treatment at 21 °C (Lee *et al.* 2009), a result that is consistent with the enlarged meristems found here for cooler temperatures given continuously. Shifts in temperature that are large and rapid could well induce a different response regime than prolonged exposure to a constant temperature.

Radial expansion rate

In roots, studies of growth are widely confined to one dimension (i.e. elongation), but growth in the other directions is far from zero and is important, for example in responses to water stress (Liang *et al.* 1997) and to compact soil (Tracy *et al.* 2012). We found that root diameter decreases more or less linearly as temperature increases but that elemental radial expansion rate is not linearly dependent on temperature (Figs. 6b, 10b). Maximal rates of elemental radial expansion at 15 and 20 °C are indistinguishable and substantially lower than at 25 °C. To our knowledge, this is the first report of radial expansion rates in the root as a function of temperature. Pahlavanian and Silk (1988) reported that, for maize, root diameter was positively correlated with temperature, the opposite of what happened here for *A. thaliana*. Perhaps, thickening in the cold represents a useful means to conserve heat for the thin roots of *A. thaliana*? Regardless, radial expansion, in contrast to elongation, fails to scale with temperature, providing further evidence supporting the claim that growth rates in orthogonal directions are regulated independently (Baskin 2005; Tsukaya 2008).

The spatial profile of elemental radial expansion rate and its response to temperature closely resembles that of cell division rate, including the non-linear dependence on temperature (Figs. 6b, 9b, 10b). There is no such resemblance for elongation: elemental elongation rate increases gradually with distance from the quiescent centre at all temperatures whereas rates of both radial expansion and cell division either decrease steadily with distance from the quiescent centre (25 and 30 °C) or remain steady for a hundred microns or so before decreasing steadily (15 and 20 °C). Evidently, the coupling in the root meristem between rates of elongation and division is flexible, allowing cell size to change (in either space or time). Comparable conclusions have been reached for leaves where division and expansion, though coordinated, appear to be appreciably independent (Granier & Tardieu 2009; Horiguchi & Tsukaya 2011; Gonzalez *et al.* 2012; Kalve *et al.* 2014). We hypothesize that, in contrast, the congruence of rates of radial expansion and cell division seen here reflect a tight mechanistic coupling; further, we suggest this might be productive to test in view of the agronomic and physiological relevance of root diameter (Jeong *et al.* 2013; Gu *et al.* 2014; Kong *et al.* 2016).

Root zonation

The root's growth zone is customarily divided into the meristem, where cells divide, and the elongation zone, where cells elongate rapidly. Here, we document kinematically the existence of a region between these zones where cells neither divide nor elongate rapidly (Fig. 3). We define the shootward terminus of the meristem as the position where cell production rate falls to zero (Fig. 9a), and the rootward terminus of the elongation zone as the location where the velocity profile changes from gradual to steep (Fig. 4). This intermediary zone was about 325 μm at 15 °C and decreased steadily in length with increasing temperature, reaching about 150 μm at 30 °C (Fig. 3). The time to traverse this region was actually similar at 15 and 20 °C (about 11 h) and slower than at 25 and 30 °C (about 8 h), times that are comparable with, but somewhat shorter than, the average cell cycle duration (Table 2).

One or even two regions between meristem and rapid elongation zone have been proposed and variously named (Ivanov & Dubrovsky 2013). However, with kinematic analysis, cell division usually extends right up to the zone of rapid elongation (e.g. Beemster & Baskin 1998; West *et al.* 2004; Bizet *et al.* 2015). We think the more rootward termination of cell production profiles found here probably reflects improved measurement of the velocity profile.

Measuring the velocity profile accurately is not trivial. The meristem has a high absolute velocity but a low divergence of velocity whereas the elongation zone has a low absolute velocity with a high divergence; measurement methods that work accurately in one regime tend to work poorly in the other. Without adequate resolution, the transition between shallow and steep velocity gradients will be smoothed out, thereby tending to increase calculated velocity values and give rise to finite cell production (Eqn 3). Despite considerable interest in developing software for automated and high-resolution analysis of the velocity profile (e.g. Walter *et al.* 2002; van der Weele *et al.* 2003; Basu *et al.* 2007; Wuyts *et al.* 2011), use of these new tools has been largely restricted to characterizing elongation.

Cell production activity terminating about 10 h (or a few hundred microns) before the onset of rapid elongation, as seen here, is consistent with meristem size determined qualitatively through methods that locate mitoses (or other cell cycle markers), which usually show the meristem terminating where cell length remains short. It is also consistent with the accumulating molecular evidence for some kind of transitional region between meristem and elongation zone (Ivanov & Dubrovsky 2013). Further research is needed into the underlying identity and function of cells in this transitional zone to determine to what extent it should be viewed as a non-proliferative conclusion to the meristem, a slowly growing introduction to the elongation zone, or a distinct chapter of root zonation.

Temperature compensation

Surprisingly, both final cell flux (i.e. the total rate of cell production) and the length of the elongation zone were essentially

insensitive to moderate temperatures (Fig. 10c). Elongation zone length varies in maize roots grown at constant temperature (Nagel *et al.* 2009) and in various species cell proliferation scales, at least approximately, with temperature (e.g. Van't Hof & Ying 1964; Silk 1992). Insofar as *A. thaliana* roots inhabit superficial layers of the soil, they might have evolved a response pattern that differs from species with deeper roots.

Be that as it may, total cell production rate here is unaffected by temperature even though, as temperature increases, the meristem shortens and has fewer cells while cell division rate increases (Fig. 9a,b). As the meristem shortens from 15 to 20 °C, the maximal (local) cell production rate increases, mainly because meristem cells are shorter (Fig. 7). As the meristem gets even shorter from 20 to 25 °C, maximal cell production rate becomes even higher, but in this case mainly, because of an increased rate of cell division (Fig. 9b). Changes in meristem length are thus compensated by changes in either cell length or division rate to maintain an invariant final cell flux. A related compensation happens in the maize leaf exposed to cold nights, where smaller meristem cells at least partly make up for slower division rates (Rymen *et al.* 2007). Similarly, we find that the elongation zone remains constant in length even though, as temperature increases, the time to traverse that zone decreases while final cell length increases. In this case, larger elemental elongation rate is compensated by faster exit from the elongation zone to keep the elongation zone length, but interestingly not cell length, roughly constant.

In leaves, compensation mechanisms have been well studied where they help keep leaf area constant (Granier & Tardieu 2009; Horiguchi & Tsukaya 2011). Here in roots, the compensating mechanisms act on the length of the elongation zone and the cumulative output of the meristem (i.e. cell flux). In a simple model, the length of the elongation zone would depend directly on cell flux: each cell entering the zone would execute an identical programme of elongation and thus the more cells entering per unit time (i.e. the larger the cell flux), the longer the elongation zone. Consistently, cell flux and the size of the elongation zone are typically correlated (e.g. Beemster & Baskin 1998; Beemster *et al.* 2002; Liu *et al.* 2013). Still, the correlation is hardly absolute (e.g. Rahman *et al.* 2007). Moreover, while the constancy of cell flux and elongation-zone length seen here extends their correlation, that this is so despite differences in underlying cell behaviour suggests that this correlation reflects not direct causality but rather coordinated responses to a common stimulus.

The existence of compensating mechanisms to maintain cell flux and elongation-zone length suggests that these parameters are unlikely to be delineated cell-autonomously. This adds experimental support to a recent theoretical demonstration showing that cell autonomous behaviour failed to realistically reproduce root zonation (De Vos *et al.* 2014). As for determining where elongation ends, Band *et al.* (2012) have developed a model where growth in the elongation zone dilutes the concentration of the hormone gibberellin so that when the concentration falls below a threshold, growth stops; incorporating known parameters relating to gibberellin signalling, the model provides a cell-autonomous means to ending elongation. However, to reproduce the invariance seen here for elongation-zone length, the model would seem to require the parameters to have a rather complex temperature dependence. As for cell division, models commonly equate the proliferative output of the root meristem with its length, but as shown here, that equivalence need not hold. In contrast to meristem length, cell production rate has been rarely modelled; the temperature compensated cell flux seen here appears to offer a useful system for discovering how the root meristem manages its manufacture of cells.

ACKNOWLEDGMENTS

This work was supported in part by the US National Institutes of Health award EB00573-01A1 to K. Palaniappan, a US National Science Foundation computing infrastructure grant CNS-1429294 to K. Palaniappan, and by a China Scholarship Council award to Xiaoli Yang. We thank Phil Wigge (Sainsbury Laboratory, UK) for the gift of *pif4/pif5* seeds, Daniele Dietrich (University of Nottingham, UK) for the gift of GTP-LTI6a seeds, Gerrit Beemster (University of Antwerp, Belgium) for Locpoly, and Lawrence Winship (Hampshire College, USA) for the non-linear curve-fitting routine. We acknowledge insightful comments on the manuscript from Dr's Beemster and Wigge and from Dr Abidur Rahman (Iwate University, Japan).

REFERENCES

Band L.R., Úbeda-Tomás S., Dyson R.J., Middleton A.M., Hodgman T.C., Owen M.R.,…, King J.R. (2012) Growth-induced hormone dilution can explain the dynamics of plant root cell elongation. *Proceedings of the National Academy of Sciences of the United States of America* **109**, 7577-7582.

Baskin T.I. (2000) On the constancy of cell division rate in the root meristem. *Plant Molecular Biology* **43**, 545–554.

Baskin T.I. (2005) Anisotropic expansion of the plant cell wall. *Annual Reviews of Cell & Developmental Biology* **21**, 203–222.

Baskin T.I. (2013) Patterns of root growth acclimation: constant processes, changing boundaries. *Wiley Interdisciplinary Reviews: Developmental Biology* **2**, 65–73.

Baskin T.I., Betzner A.S., Hoggart R., Cork A. & Williamson R.E. (1992) Root morphology mutants in *Arabidopsis thaliana*. *Australian Journal of Plant Physiology* **19**, 427–437.

Baskin T.I. & Wilson J.E. (1997) Inhibitors of protein kinases and phosphatases alter root morphology and disorganize cortical microtubules. *Plant Physiology* **113**, 493–502.

Basu P., Pal A., Lynch J.P. & Brown K.M. (2007) A novel image-analysis technique for kinematic study of growth and curvature. *Plant Physiology* **145**, 305–316.

Beemster G.T.S. & Baskin T.I. (1998) Analysis of cell division and elongation underlying the developmental acceleration of root growth in *Arabidopsis thaliana*. *Plant Physiology* **116**, 1515–1526.

Beemster G.T.S., De Vusser K., De Tavernier E., De Bock K. & Inzé D. (2002) Variation in growth rate between arabidopsis ecotypes is correlated with cell division and A-type cyclin-dependent kinase activity. *Plant Physiology* **129**, 854–864.

Ben-Haj-Salah H. & Tardieu F. (1995) Temperature affects expansion rate of maize leaves without change in spatial distribution of cell length. Analysis of the coordination between cell division and cell expansion. *Plant Physiology* **109**, 861–870.

Bizet F., Hummel I. & Bogeat-Triboulot M.B. (2015) Length and activity of the root apical meristem revealed *in vivo* by infrared imaging. *Journal of Experimental Botany* **66**, 1387–1395.

De Vos D., Vissenberg K., Broeckhove J. & Beemster G.T.S. (2014) Putting theory to the test: which regulatory mechanisms can drive realistic growth of a root? *PLoS Computational Biology* **10**e1003910.

© 2016 John Wiley & Sons Ltd,

Dong G., Baskin T. I. & Palaniappan K (2006) Motion flow estimation from image sequences with applications to biological growth and motility. *IEEE International Conference on Image Processing*, pp 1245-1248.

Erickson R.O. (1959) Integration of plant growth processes. *American Naturalist* **93**, 225–235.

Erickson R.O. (1976) Modeling of plant growth. *Annual Reviews of Plant Physiology* **27**, 407–434.

Fiorani F. & Beemster G.T.S. (2006) Quantitative analyses of cell division in plants. *Plant Molecular Biology* **60**, 963–979.

Franklin K.A., Toledo-Ortiz G., Pyott D.E. & Halliday K.J. (2014) Interaction of light and temperature signalling. *Journal of Experimental Botany* **65**, 2859–2871.

Gonzalez N., Vanhaeren H. & Inzé D. (2012) Leaf size control: complex coordination of cell division and expansion. *Trends in Plant Science* **17**, 332–340.

Granier C., Massonnet C., Turc O., Muller B., Chenu K. & Tardieu F. (2002) Individual leaf development in *Arabidopsis thaliana*: a stable thermal-time-based programme. *Annals of Botany* **89**, 595–604.

Granier C. & Tardieu F. (1998) Is thermal time adequate for expression the effects of temperature on sunflower leaf development? *Plant, Cell & Environment* **21**, 695–703.

Granier C. & Tardieu F. (2009) Multi-scale phenotyping of leaf expansion in response to environmental changes: the whole is more than the sum of parts. *Plant, Cell & Environment* **32**, 1175–1184.

Gray W.M., Östin A., Sandberg G., Romano C.P. & Estelle M. (1998) High temperature promotes auxin-mediated hypocotyl elongation in arabidopsis. *Proceedings of the National Academy of Sciences of the United States of America* **95**, 7197–7202.

Grebe M., Xu J., Möbius W., Ueda T., Nakano A., Geuze H.J., Rook M.B. & Scheres B. (2003) Arabidopsis sterol endocytosis involves actin-mediated trafficking via ARA6-positive early endosomes. *Current Biology* **13**, 1378–1387.

Green P.B. (1976) Growth and cell pattern formation on an axis: critique of concepts, terminology and modes of study. *Botanical Gazette* **137**, 187–202.

Grif V.G., Ivanov V.B. & Machs E.M. (2002) Cell cycle and its parameters in flowering plants. *Tsitologia* **44**, 936–980.

Gu J., Xu Y., Dong X., Wang H. & Wang Z. (2014) Root diameter variations explained by anatomy and phylogeny of 50 tropical and temperate tree species. *Tree Physiology* **34**, 415–425.

Hanzawa T., Shibasaki K., Numata T., Kawamura Y., Gaude T. & Rahman A. (2013) Cellular auxin homeostasis under high temperature is regulated through a SORTING NEXIN1-dependent endosomal trafficking pathway. *The Plant Cell* **25**, 3424–3433.

Horiguchi G. & Tsukaya H. (2011) Organ size regulation in plants: insights from compensation. *Frontiers in Plant Science* **2**, 24.

Ivanov V.B. & Dubrovsky J.G. (2013) Longitudinal zonation pattern in plant roots: conflicts and solutions. *Trends in Plant Science* **18**, 237–243.

Jeong J.S., Kim Y.S., Redillas M.C.F.R., Jang G., Jung H., Bang S.W., … Kim J.K. (2013) *OsNAC5* overexpression enlarges root diameter in rice plants leading to enhanced drought tolerance and increased grain yield in the field. *Plant Biotechnology Journal* **11**, 101–114.

Kalve S., Fotschki J., Beeckman T., Vissenberg K. & Beemster G.T.S. (2014) Three-dimensional patterns of cell division and expansion throughout the development of *Arabidopsis thaliana* leaves. *Journal of Experimental Botany* **65**, 6385–6397.

Koini M.A., Alvey L., Allen T., Tilley C.A., Harberd N.P., Whitelam G.C. & Franklin K.A. (2009) High temperature-mediated adaptations in plant architecture require the bHLH transcription factor PIF4. *Current Biology* **19**, 408–413.

Kong D.L., Wang J.J., Kardol P., Wu H.F., Zeng H., Deng X.B. & Deng Y. (2016) Economic strategies of plant absorptive roots vary with root diameter. *Biogeosciences* **13**, 415–424.

Kumar S.V., Lucyshyn D., Jaeger K.E., Alós E., Alvey E., Harberd N.P. & Wigge P.A. (2012) Transcription factor PIF4 controls the thermosensory activation of flowering. *Nature* **484**, 242–245.

Lee Y.P., Fleming A.J., Körner C. & Meins F. Jr. (2009) Differential expression of the CBF pathway and cell cycle-related genes in Arabidopsis accessions in response to chronic low-temperature exposure. *Plant Biology* **11**, 273–283.

Liang B.M., Sharp R.E. & Baskin T.I. (1997) Regulation of growth anisotropy in well-watered and water-stressed maize roots. I. Spatial distribution of longitudinal, radial, and tangential expansion rates. *Plant Physiology* **115**, 101–111.

Liu Y., Lai N., Gao K., Chen F., Yuan L. & Mi G. (2013) Ammonium inhibits primary root growth by reducing the length of meristem and elongation zone and decreasing elemental expansion rate in the root apex in *Arabidopsis thaliana*. *PLoS ONE* **8**e61031.

Lorrain S., Allen T., Duek P.D., Whitelam G.C. & Fankhauser C. (2008) Phytochrome-mediated inhibition of shade avoidance involves degradation of growth-promoting bHLH transcription factors. *The Plant Journal* **53**, 312–323.

Nagel K.A., Kastenholz B., Jahnke S., van Dusschoten D., Aach T., Mühlich M., … Schurr U. (2009) Temperature responses of roots: impact on growth, root system architecture and implications for phenotyping. *Functional Plant Biology* **36**, 947–959.

Nakamura Y., Wakabayashi K., Kamisaka S. & Hoson T. (2002) Effects of temperature on the cell wall and osmotic properties in dark-grown rice and azuki bean seedlings. *Journal of Plant Research* **115**, 455–461.

Nelissen H., Rymen B., Coppens F., Dhondt S., Fiorani F. & Beemster G.T.S. (2013) Kinematic analysis of cell division in leaves of mono- and dicotyledonous species: a basis for understanding growth and developing refined molecular sampling strategies. *Methods in Molecular Biology* **959**, 247–264.

Nieto C., López-Salmerón V., Davière J.M. & Prat S. (2015) ELF3-PIF4 interaction regulates plant growth independently of the Evening Complex. *Current Biology* **25**, 187–193.

Pahlavanian A.M. & Silk W.K. (1988) Effect of temperature on spatial and temporal aspects of growth in the primary maize root. *Plant Physiology* **87**, 529–532.

Palaniappan K., Jiang H.S. & Baskin T.I. (2004) *Non-Rigid Motion Estimation Using The Robust Tensor Method*, pp. 25–33. *IEEE Computer Vision & Pattern Recognition Workshop on Articulated and Nonrigid Motion*. IEEE Computer Society, Washington DC.

Parent B. & Tardieu F. (2012) Temperature responses of developmental processes have not been affected by breeding in different ecological areas for 17 crop species. *New Phytologist* **194**, 760–774.

Parent B., Turc O., Gibon Y., Stitt M. & Tardieu F. (2010) Modelling temperature-compensated physiological rates, based on the co-ordination of responses to temperature of developmental processes. *Journal of Experimental Botany* **61**, 2057–2069.

Peters W.S. & Baskin T.I. (2006) Tailor-made composite functions as tools in model choice: the case of sigmoidal vs bi-linear growth profiles. *Plant Methods* **2**, 11.

Pritchard J., Barlow P.W., Adam J.S. & Tomos A.D. (1990) Biophysics of the inhibition of the growth of maize roots by lowered temperature. *Plant Physiology* **93**, 222–230.

Rahman A., Bannigan A., Sulaman W., Pechter P., Blancaflor E.B. & Baskin T.I. (2007) Auxin, actin and growth of the *Arabidopsis thaliana* primary root. *The Plant Journal* **50**, 514–528.

Rasband W.S. (2015) ImageJ. U. S. National Institutes of Health, Bethesda, Maryland, USA. http://imagej.nih.gov/ij/.

Rymen B., Fiorani F., Kartal F., Vandepoele K., Inzé D. & Beemster G.T.S. (2007) Cold nights impair leaf growth and cell cycle progression in maize through transcriptional changes of cell cycle genes. *Plant Physiology* **143**, 1429–1438.

Silk W.K. (1992) Steady form from changing cells. *International Journal of Plant Sciences* **153**, S49–S58.

Silk W.K. & Abou Haidar S. (1986) Growth of the stem of *Pharbitis nil*: analysis of longitudinal and radial components. *Physiologie Végétale* **24**, 109–116.

Stavang J.A., Gallego-Bartolomé J., Gómez M.D., Yoshida S., Asami T., Olsen J. E., … Blázquez M.A. (2009) Hormonal regulation of temperature-induced growth in arabidopsis. *The Plant Journal* **60**, 589–601.

Sultan S.E. (2000) Phenotypic plasticity for plant development, function and life history. *Trends in Plant Science* **5**, 537–542.

Sun J., Qi L., Li Y., Chu J. & Li C. (2012) PIF4-mediated activation of *YUCCA8* expression integrates temperature into the auxin pathway in regulating arabidopsis hypocotyl growth. *PLoS Genetics* **8**e1002594.

Tardieu F. & Granier C. (2000) Quantitative analysis of cell division in leaves: methods, developmental patterns and effects of environmental conditions. *Plant Molecular Biology* **43**, 555–567.

Tracy S.R., Black C.R., Roberts J.A., Sturrock C., Mairhofer S., Craigon J. & Mooney S.J. (2012) Quantifying the impact of soil compaction on root system architecture in tomato (*Solanum lycopersicum*) by X-ray micro-computed tomography. *Annals of Botany* **110**, 511–519.

Trudgill D.L., Honek A., Li D. & Van Staalen N.M. (2005) Thermal time -- concepts and utility. *Annals of Applied Biology* **146**, 1–14.

Tsukaya H. (2008) Controlling size in multicellular organs: focus on the leaf. *PLoS Biology* **6**e174.

van der Weele C.M., Jiang H.S., Palaniappan K.K., Ivanov V.B., Palaniappan K. & Baskin T.I. (2003) A new algorithm for computational image analysis of deformable motion at high spatial and temporal resolution applied to root

© 2016 John Wiley & Sons Ltd,

growth. Roughly uniform elongation in the meristem and also, after an abrupt acceleration, in the elongation zone. *Plant Physiology* **132**, 1138–1148.

Van't Hof J. & Ying H.K. (1964) Relationship between the duration of the mitotic cycle, the rate of cell production and the rate of growth of Pisum roots at different temperatures. *Cytologia* **29**, 399–406.

Walter A., Spies H., Terjung S., Küsters R., Kirchgessner N. & Schurr U. (2002) Spatio-temporal dynamics of expansion growth in roots: automatic quantification of diurnal course and temperature response by digital image sequence processing. *Journal of Experimental Botany* **53**, 689–698.

Webster P.L. & MacLeod R.D. (1980) Characteristics of root apical meristem population kinetics: a review of analyses and concepts. *Environmental and Experimental Botany* **20**, 335–358.

West G., Inzé D. & Beemster G.T.S. (2004) Cell cycle modulation in the response of the primary root of arabidopsis to salt stress. *Plant Physiology* **135**, 1050–1058.

Wuyts N., Bengough A.G., Roberts T.J., Du C., Bransby M.F., McKenna S.J. & Valentine T.A. (2011) Automated motion estimation of root responses to sucrose in two *Arabidopsis thaliana* genotypes using confocal microscopy. *Planta* **234**, 769–784.

Yazdanbakhsh N. & Fisahn J. (2010) Analysis of *Arabidopsis thaliana* root growth kinetics with high temporal and spatial resolution. *Annals of Botany* **105**, 783–791.

Zhu J., Zhang K.X., Wang W.S., Gong W., Liu W.C., Chen H.G., Xu H.H. & Lu Y.T. (2015) Low temperature inhibits root growth by reducing auxin accumulation via *ARR1/12*. *Plant & Cell Physiology* **56**, 727–736.

Received 15 September 2016; received in revised form 26 October 2016; accepted for publication 31 October 2016

SUPPORTING INFORMATION

Additional Supporting Information may be found in the online version of this article at the publisher's web-site.

The Stripflow program is available here: https://github.com/TobiasBaskin/Stripflow-release

© 2016 John Wiley & Sons Ltd, *Plant, Cell and Environment*